The Reaction of Cu(I) (^{1}S and ^{3}D) with N_2O: An ab Initio Study

Annelies Delabie and Kristine Pierloot*

Department of Chemistry, University of Leuven, Celestijnenlaan 200F, B-3001 Heverlee-Leuven, Belgium

Received: December 18, 2001; In Final Form: March 19, 2002

The reactions of ^{1}S and ^{3}D Cu^+ ions with N_2O are studied by means of ab initio methods. The structure of all stationary points along the reaction coordinate is optimized with density functional theory (DFT), using the B3LYP functional. The reaction and binding energies and the activation barriers are evaluated with DFT-B3LYP and also with the coupled cluster method CCSD(T). Three reaction paths were found, depending on the orientation of the approaching N_2O molecule. If N_2O approaches the Cu^+ ions via its O-side, this leads to formation of CuO^+ and N_2. On the other hand, if N_2O attacks via its N-end, the reaction products are CuN_2^+ and an O atom. Finally, it was found that the ^{3}D Cu^+ ions can also react with the central N of N_2O, with formation of the insertion product $[OCuN_2]^+$. The most exothermic path is the insertion reaction of Cu^+ into the N_2-O bond. The calculations indicate that bare ^{1}S Cu^+ ions are relatively inert with respect to N_2O: high energy barriers are calculated. The ^{3}D Cu^+ ions, on the other hand, are strong activators of the N_2-O bond, and the reactions proceed without energy barrier, in agreement with experiment.

1. Introduction

Because they can provide fundamental information about catalytic bond activation a large number of studies—both experimental and theoretical—have been devoted to the reactions of transition metal atoms or ions with small molecules.[1−12] Many of these studies concentrated on the activation of hydrocarbons (CH_4, CH_2, C_2H_4, ...), NH_3, amines, H_2O, and alcohols. Wide attention was also given to the activation of the C−O and N−O bonds in some important pollutants of the atmosphere (NO, CO, NO_2, CO_2, and N_2O). The reactions of all transition metal atoms of the first series with N_2O have been studied both by theory and experiment.[2,5,13−24] Although some transition metal ion−N_2O reactions have been investigated experimentally,[11,12] none of them were so far studied by means of theoretical methods. Fundamental insight in the interaction and reaction of transition metal ions with N_2O is important for the eludication of the origin of a number of catalytic decomposition reactions. Many heterogeneous catalysts for the decomposition of N_2O have been reported, including supported and unsupported transition metals, pure and mixed oxides, and zeolitic systems containing transition metal ions.[25] Generally, it is observed that, of the first row transition metals, Co and Cu exhibit a very high activity.[25]

This paper will present a theoretical investigation of the gas-phase reactions of Cu(I) ions with N_2O. The reactions of ground state ^{1}S and excited state ^{3}D Cu(I) ions with N_2O have recently been studied by guided ion beam mass spectrometry. [11] Four reaction products were observed: CuO^+, CuN_2^+, CuN^+, and NO^+. The dominant reaction paths result from cleavage of the weak N_2-O bond, followed by binding one of the fragments to Cu^+:

$$Cu^+ + N_2O \rightarrow CuO^+ + N_2 \quad (1)$$

$$Cu^+ + N_2O \rightarrow CuN_2^+ + O \quad (2)$$

Both reactions are endothermic and spinforbidden for the ground state ^{1}S Cu^+ ions. However, they become exothermic and without spin restrictions for ^{3}D Cu^+ ions, where no reaction barriers were observed.[11] Accurate kinetic information about these reactions is still missing in the literature; the reaction mechanism is suggested to be complex. Furthermore, the error bars on the reported reaction energies, both theoretical and experimental, are usually large. For instance, the experimental dissociation energy of $[CuN_2]^+$, formed in reaction 2, 21 kcal/mol, contains an uncertainty of about 7 kcal/mol.[11] Theoretical estimates have, according to the best of our knowledge, not yet been made. Another example is the dissociation energy of CuO^+, which was recently determined by experiment (31 kcal/mol) with an accuracy of 3 kcal/mol.[11] Theoretical studies, on the other hand, report strongly deviating results at different levels of theory.[9,26]

In this work, theoretical methods have been applied to investigate the reactions of Cu^+ (^{1}S and ^{3}D) with N_2O. We have not only studied the formation of CuO^+ and $[CuN_2]^+$ but also a third possibility, namely, the insertion reaction of Cu^+ in the O−N bond of N_2O:

$$Cu^+ + N_2O \rightarrow [OCuN_2]^+ \quad (3)$$

Both the reaction energies and energy barriers will be evaluated for reactions 1−3.

2. Theoretical Methods

Geometry optimizations were performed by using density functional theory (DFT) with the B3LYP functional. The basis set used consists of the relativistic effective core potentials (ECP) of Dolg on Cu, in which the 3s, 3p, 3d, and 4s electrons are treated explicitly by a (8s7p6d) Gaussian basis set contracted to [6s5p3d].[27] This ECP for Cu was combined with the triple-ζ basis sets of Ahlrichs for N and O,[28] augmented with two d- and one f-polarization functions, denoted as TZV(2P). The choice of this particular basis set for optimizing the structures was made after performing test calculations on the reagents and products of reactions 1−3. The importance of the polarization

* Corresponding author. Fax: +32-16 32 79 92. E-mail: Kristin.Pierloot@chem.kuleuven.ac.be.

10.1021/jp014569d CCC: $22.00
Published on Web 05/17/2002

functions on N,O and the incorporation of relativistic effects by means of the ECP on Cu will be discussed in section 3.1. The unrestricted DFT formalism was employed for the open-shell systems. All stationary points were characterized by vibrational analysis and the ZPE (zero-point vibrational energy) was calculated. The transition state structures all represent saddlepoints, characterized by one negative eigenvalue of the Hessian matrix. The intrinsic reaction coordinate (IRC) was then calculated, starting from the transition state structure in the direction of both reagents and products, to probe the reaction path and check if the correct transition state was located.[29] Atomic charges and spin densities were provided by Mulliken population analysis, and the Mulliken orbital populations were checked.

To evaluate the reaction and binding energies and activation barriers, we have also performed coupled cluster single-point calculations using the two sets of B3LYP structures. The Douglas−Kroll formalism was used to calculate the relativistic corrections at the CCSD(T) level. For these calculations, a new relativistic basis set for Cu has been constructed by using exactly the same procedure as in ref 24, but including relativistic effects by means of the Douglas−Kroll method. This basis set also describes 3p−3d intershell correlation effects.[24,30] The number of contracted functions used in the CCSD(T) calculations was [7s6p5d2f1g]. For N and O, we used the (14s9p4d3f)/[4s3p2s1f] contractions from the MOLCAS ANO-L library,[31] denoted in the following text as small ANO. For the calculations of the reaction and/or binding energies involving the N_2O, N_2, O, Cu^+, CuO^+, $[CuN_2]^+$, and $[OCuN_2]^+$ species, it was possible to use even larger ANO-L basis sets on O and N, namely the (14s9p4d3f)/[5s4p3d1f] contractions (denoted as large ANO). The CCSD(T) reference wave function was obtained by performing a ROHF (restricted open-shell Hartree−Fock) calculation. In the subsequent CCSD(T) calculations, the Cu 3s, 3p, 3d, and 4s and N,O 2s and 2p electrons were considered in the correlation treatment. Finally, we have added the ZPE, calculated with DFT, to the coupled cluster energies.

All DFT calculations were perfomed using the GAUSSIAN 98 package,[32] while the CCSD(T) calculations were carried out with MOLCAS-5.0.[33]

3. Results and Discussion

First, the reaction energies will be considered, to identify the most stable reaction products. Next, the reaction mechanisms and energy barriers will be discussed.

3.1. Reaction Energies. The structures of all reagents and products of reactions 1−3 are represented in Figure 1. They were obtained by means of the DFT-B3LYP method in combination with three types of basis sets. First, we have used TZVP basis sets for all atoms. Next, we replaced the TZVP basis set of Cu by the ECP, to examine the importance of relativistic effects on the structures. Next, the Cu ECP was combined with TZV(2P) basis sets on O,N. As one can see, the choice of the basis sets has a significant effect on the structures, at least for systems containing Cu. All Cu-ligand bond distances decrease significantly when including relativistic effects. For instance, the $Cu-O^+$ bond length reduces from 1.818 to 1.792 Å. The addition of more polarization functions to the basis sets on O and N also has a substantial effect on the structures. The $Cu-O^+$ bond length further reduces to 1.775 Å. This DFT-B3LYP bond distance is still longer than that previously obtained with MR−SDCI (multireference singles and doubles configuration interaction) and comparible basis sets, yielding a bond distance of 1.678 Å.[26]

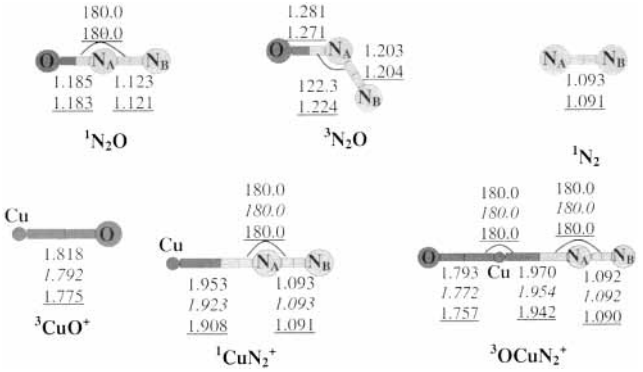

Figure 1. DFT-B3LYP structures of the reagents and reaction products of the Cu^+-N_2O reactions. Bond distances are given in angstroms, bond angles in degrees. The upper, middle (in italics), and lower (underlined) values indicate geometrical parameters obtained with different basis sets: TZV(P), Cu(ECP)-N,O(TZVP), and Cu(ECP)-N,O-(TZV(2P)), respectively.

The B3LYP/ECP-TZV(2P) reaction energies of reactions 1−3 are reported in Table 1, together with the CCSD(T)/ANO results, calculated using the B3LYP/ECP-TZV(2P) structures. As one can see, significant differences were obtained for the reaction energies at different levels of theory. We will first consider the reactions 1 and 2. In agreement with the experimental findings of Rodgers et al.,[11] both theoretical methods indicate that the formation of both CuO^+ and $[CuN_2]^+$ is endothermic for $^1Cu^+$ ions but becomes exothermic for $^3Cu^+$. However, which of the two species will be formed preferentially depends on the method: DFT clearly points to the formation of CuO^+ as the most favorable reaction product, whereas CCSD(T) predicts similar reaction energies for both reactions.

The above reaction energies are determined by the theoretical binding energies of N_2O, CuO^+, and CuN_2^+, respectively, and by the Cu^+ singlet−triplet excitation energy. These four energies are also reported in Table 1. The N_2-O binding energy is overestimated by 3 kcal/mol with DFT-B3LYP. We note that the DFT-B3LYP value is much closer to experiment (39.9 kcal/mol) than a previous theoretical estimate, 59 kcal/mol, obtained recently with DFT-BP86.[36] CCSD(T), on the other hand, underestimates the experimental binding energy by more than 6 kcal/mol. The CCSD(T) results could not be improved by extending the O,N basis sets to (5s4p3d2f). On the other hand, the presence of at least one f-function on O,N is crucial for the description of the N_2-O binding energy: without f-functions on O,N the calculated binding energy reduces to 27.7 kcal/mol.

The calculated reaction energies for the formation of $[CuN_2]^+$ range between −22.2 and −24.5 kcal/mol, depending on the level of theory. In this case both DFT and CCSD(T) results are in good agreement with the experimental estimate for the dissociation energy of $[CuN_2]^+$, i.e., 21.2 (± 7) kcal/mol.[11] On the other hand, for the binding energies of CuO^+, DFT results predict a much larger value (33.1 kcal/mol) than CCSD(T) (23.1−23.4 kcal/mol). The most recent experimental estimate for the CuO^+ binding energy is 31.1 (± 3) kcal/mol,[11] in agreement with the DFT results. The fact that the CCSD(T) method does not perform well for the CuO^+ binding energy was already noted in previous theoretical studies,[9,37] where even lower binding energies were reported: 19.4[9] and 16.7 kcal/mol,[37] respectively. The large difference between these previous and the present CCSD(T) results is largely due to the absence of relativistic corrections in the earlier studies: without the Douglas-Kroll approximation (and using the nonrelativistic alternative for the ANO-L basis set on Cu) we also calculate a

TABLE 1: Reaction Energies (kcal/mol) for Reactions of Cu^+ with N_2O at the DFT-B3LYP Level and with CCSD(T)

		CCSD(T) (method)		
	B3LYP (method) ECP-TZV(2P) (basis)	small ANO (basis)	large ANO (basis)	exptl (method)
$^1N_2 + {}^3O \rightarrow {}^1N_2O$	−43.1	−35.2	−34.5	−39.9[a]
$^1Cu^+ + {}^3O \rightarrow {}^3CuO^+$	−33.1	−23.4	−23.1	−31.1 ± 3[b]
$^1Cu^+ + {}^1N_2 \rightarrow {}^1CuN_2^+$	−24.5	−23.5	−22.9	−21.2 ± 7[b]
$^1CuN_2^+ + {}^3O \rightarrow {}^3[OCuN_2]^+$	−36.6	−29.4	−28.9	
$^3CuO^+ + {}^1N_2 \rightarrow {}^3[OCuN_2]^+$	−28.1	−29.6	−28.7	
$^1Cu^+ \rightarrow {}^3Cu^+$	+56.2	+63.6	+63.3	+64[c]
$^1Cu^+ + {}^1N_2O \rightarrow {}^3CuO^+ + {}^1N_2$	+10.0	+11.8	+11.4	+8.8[d]
$^3Cu^+ + {}^1N_2O \rightarrow {}^3CuO^+ + {}^1N_2$	−46.1	−51.8	−52.3	−52.6[e]
$^1Cu^+ + {}^1N_2O \rightarrow {}^1CuN_2^+ + {}^3O$	+18.6	+11.7	+11.6	+18.7[f]
$^3Cu^+ + {}^1N_2O \rightarrow {}^1CuN_2^+ + {}^3O$	−37.6	−51.9	−52.0	−45.3[g]
$^1Cu^+ + {}^1N_2O \rightarrow {}^3[OCuN_2]^+$	−18.1	−17.7	−17.3	
$^3Cu^+ + {}^1N_2O \rightarrow {}^3[OCuN_2]^+$	−74.2	−81.3	−80.9	

[a] From ref 34. [b] From ref 11. [c] From ref 35. [d] From the binding energies of N_2O and CuO^+. [e] From the binding energies of N_2O and CuO^+ and the Cu^+ $^1S-{}^3D$ energy difference. [f] From the binding energies of N_2O and CuN_2^+. [g] From the binding energies of N_2O and CuN_2^+ and the Cu^+ $^1S-{}^3D$ energy difference.

significantly (4.8 kcal/mol) lower CCSD(T) binding energy: 18.3 kcal/mol. On the other hand, using B3LYP with the nonrelativistic TZVP basis sets gives a binding energy of 29.6 kcal/mol, a reduction of 3.5 kcal/mol as compared to the ECP-TZV(2P) result included in Table 1 (but note that this difference is now due to a combination of basis set and relativistic effects).

The failure of the single reference based CCSD(T) method in describing the bonding in CuO^+ points to the occurrence of a certain amount of multiconfigurational character in the ground state of this molecule. This is conform with the isoelectronic neutral NiO molecule, which was discussed in detail in a previous study by Bauschlicher,[38] and was shown there to be inadequately described by single reference techniques too. However, even multireference methods have so far not provided an accurate result for the CuO^+ binding energy.[26] At the MR−SDCI level a value of 22.0 kcal/mol was obtained previously (including a Davidson correction), whereas a multireference perturbation treatment gave a too high value of 36.9 kcal/mol (both results included relativistic corrections by means of a relativistic ECP on Cu). In a more extended study of the first transition row neutral and monopositive oxides we have attempted to improve on these results by employing multiconfigurational perturbation theory (CASPT2) based on a large CASSCF wave function.[39] The calculated CuO^+ binding energy (with the large ANO basis set combination) is 26.5 kcal/mol (including a zero-point energy correction of 0.8 kcal/mol). Even if this is the best result obtained so far using ab initio correlated methods it is still more than 4 kcal/mol below the experimental value. Apparently, the description of CuO^+ and other transition metal oxides still remains a challenge to computational chemistry.

Subtracting the binding energy of N_2O from the binding energies of CuO^+ and $[CuN_2]^+$ yields the reaction energies of reactions 1 and 2 respectively. It follows that the reaction energies are in good agreement with experiment in the case of DFT and in reasonable agreement for CCSD(T). The reaction energy of reaction 1 at the CCSD(T) level is also in good agreement with experiment. However, this is only due to a fortuitous cancellation of errors on the CuO^+ and N_2O binding energies, which are both underestimated. We conclude that DFT, in combination with the Cu ECP and O,N TZV(2P) basis sets, generates the most accurate reaction energies for $^1Cu^+$, and that the formation of CuO^+ is thus thermodynamically more favorable than the formation of $[CuN_2]^+$.

However, both theoretical methods indicate that the most stable reaction products of the Cu^+-N_2O reactions are not CuO^+ or $[CuN_2]^+$, but the $^3[OCuN_2]^+$ adduct. The insertion of Cu^+ into the $O-N_2$ bond (reaction) is exothermic even for ground state $^1Cu^+$ ions, by about 18 kcal/mol. The structure of the $^3[OCuN_2]^+$-complex, shown in Figure 1, is linear. A linear structure was also calculated previously for the isoelectronic $^3[OCuCO]^+$ species.[9] These inserted structures both can be viewed as arising from an electrostatic interaction between CuO^+ and N_2 or CO, respectively. As one can see from the results in Table 1, the binding energy of O in $[OCuN_2]^+$ is slightly larger than the binding energy of O in CuO^+. The strengthening of the Cu−O bond by complexation with N_2 is also reflected in the structure: the Cu−O bond length decreases from 1.775 Å in CuO^+ to 1.757 Å in $[OCuN_2]^+$. A similar observation was made for the Cu−O bond in $[OCuCO]^+$. [9] It was explained there by the fact that both O and CO share the cost of the sdσ hybridization. This reduces the charge density on both sides of the Cu-atom, and enhances the electrostatic contribution to the Cu−O bond. The binding energies indicate that the Cu−N bond is also strengthened upon complexation with O, although this is not reflected in the structure: the Cu−N bond distance is longer in $[OCuN_2]^+$ (1.942 Å) than in $[CuN_2]^+$ (1.908 Å). Unfortunately, there are no experimental data to compare the reaction and binding energies involving $^3[OCuN_2]^+$. The reaction energy of the inserted $[OCuCO]^+$ is highly endothermic both for singlet and triplet Cu^+,[9] due to the much stronger binding energy of C−O in CO_2, as compared to N−O in the N_2O molecule.

The calculated singlet−triplet excitation energies in the free Cu^+ ion are also mentioned in Table 1. In this case, CCSD(T) clearly performes better than DFT. DFT underestimates the singlet−triplet splitting by 8 kcal/mol. As a consequence, the reaction energies involving $^3Cu^+$ ions are all less exothermic at the DFT level than predicted both by experiment and by CCSD(T).

3.2. Reaction Mechanisms and Energy Barriers. In the next sections, the reaction paths of reactions 1−3 will be considered. In all DFT-B3LYP calculations, we have used the Cu ECP combined with TZV(2P) basis sets on O,N. As the CCSD(T) reaction energies (see section 3.1 and Table 1) were found to be similar for both ANO basis sets used, we have chosen the smaller basis sets for the calculation of binding energies and energy barriers encountered along the reaction coordinates.

As will be shown in the following text, three distinct reaction courses may be followed when Cu^+ reacts with N_2O, depending on the orientation of the approaching N_2O with respect to Cu^+. Attack via O leads to formation of CuO^+ and N_2 (reaction (1)).

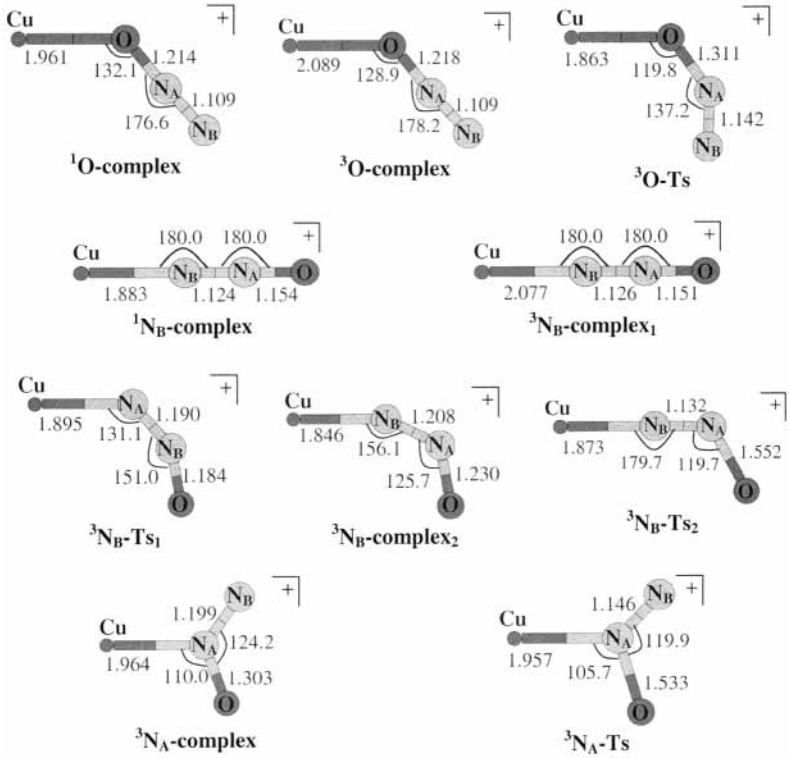

Figure 2. DFT-B3LYP structures of the Cu−N_2O-complexes and the transition states along the reaction paths for reactions 1−3. The basis sets used are Cu(ECP)-N,O(TZV(2P)). Bond distances are given in angstroms, bond angles in degrees. For the labeling of the various Cu−N_2O-complexes and transition state structures, see also the reaction schemes in Figure 3.

On the other hand, if N_2O approaches via its N-end the reaction products are CuN_2^+ and an O atom (reaction (2)). Finally, we found that Cu^+ atoms in the ^3D state can also react with N_2O via the central nitrogen, leading to insertion of Cu^+ in the O−N_2 bond, with formation of $[OCuN_2]^+$ (reaction (3)).

The calculated reaction schemes are presented in Figure 3. The structures of all stationary points along the reaction path can be found in Figures 1 and 2. The labels given to the different complexes and transition state structures indicate the orientation of O−N_A−N_B with respect to Cu^+. For instance, ^{3}O-Ts points to a transition state structure on the triplet surface in which N_2O interacts with Cu^+ via its O-side.

$^3Cu^+ + {}^1N_2O \rightarrow {}^3CuO^+ + {}^1N_2$. As already discussed in section 3.1, the reaction of $^3Cu^+$ ions is exothermic and spin-allowed. The reaction mechanism of the $^3Cu^+$−N_2O reaction is similar to that of ^{2}Cu atoms with N_2O. [24] First, a $^3[Cu{-}ON_2]^+$-complex is formed (denoted as ^{3}O-complex in Figure 2). This complex has a much larger binding energy (−24 kcal/mol) than that of the neutral [Cu−ON_2]-complex (−1 kcal/mol), mainly because of stronger electrostatic forces.[24] As in the neutral [Cu−ON_2]-complex, the O−N_A−N_B system remains linear, but the Cu−O−N_A angle is bent. These structural parameters can be rationalized by looking at the orbital interactions between the $^3Cu^+$ ($3d^94s^1$) ion and N_2O, shown in Figure 4 (for the ^{3}O-Ts (see further), but they are qualitatively the same for the ^{3}O-complex). Apart from a small contribution from electrostatic and polarization terms, the primary reason for the bent Cu−O−N_A angle is a σ electron donating interaction between the N_2O HOMO and the (singly occupied) Cu^+ $3d_z^2$ orbital (see Figure 4A). On the other hand, the interaction between the Cu 4s orbital and in-plane N_2O LUMO, which could bring about back-donation (see Figure 4B), is still weak in the initial complex. A second, completely linear, O-side complex was also optimized by imposing $C_{\infty v}$ symmetry in the geometry optimization, but was found to be a transition state on the potential energy surface, 6 kcal/mol higher in energy than the ^{3}O-complex. In a linear structure the above interactions between the $3d_z^2$,4s orbitals and the N_2O HOMO,LUMO (symmetry forbidden within $C_{\infty v}$) are replaced by an interaction with the N_2O σ lone pair. However, this interaction is much weaker: the N_2O σ lone pair, plotted in Figure 4C, has only a small contribution on O, with a much larger lobe at the N-end of N_2O.

The transition state structure for the $^3Cu^+$−N_2O reaction, denoted as ^{3}O-Ts, is also shown in Figure 2. In this structure, the Cu−O bond is shortened as compared to the ^{3}O-complex, and the O−N_A distance is increased. One can see that not only the Cu−O−N_A but also the O−N_A−N_B angle is bent at the transition state. It has been shown in previous theoretical studies on transition metal−N_2O reactions[23,24] that the bending of the N_2O system is an indication that charge is transferred from the transition metal toward the N_2O LUMO.[23,24] Such a charge transfer also occurs in the present Cu^+ transition state structure. Next to the charge donation from the in-plane N_2O HOMO to the singly occupied d_z^2 orbital of $^3Cu^+$ (see Figure 4B), there occurs back-donation from the 4s Cu^+ orbital toward the in-plane N_2O LUMO. This initiates the bending of N_2O. The two charge transfers proceed in opposite directions, but they have about the same magnitude in the transition state structure. Thus, there is no netto charge transfer at the ^{3}O-Ts. This is in contrast to the Cu atom−N_2O reaction, where the back-donation clearly overrules the donation, with as a result a charge transfer from Cu toward N_2O at the transition state structure.[24] The two opposite electron transfers become more and more pronounced as the reaction proceeds, so that the electronic configuration of Cu(I) gradually changes from $3d^94s^1$ to $3d^{10}4s^0$. As such, the spin density gradually shifts toward O while the Cu charge almost remains constant. The O−N bond is broken and $^3CuO^+$ is formed. Its $^3\Sigma^-$ ground state can indeed be viewed as resulting from the interaction between ground-state Cu^+ (^{1}S, $3d^{10}$) and ground-state O (^{3}P).[40] The energy barrier, calculated as the

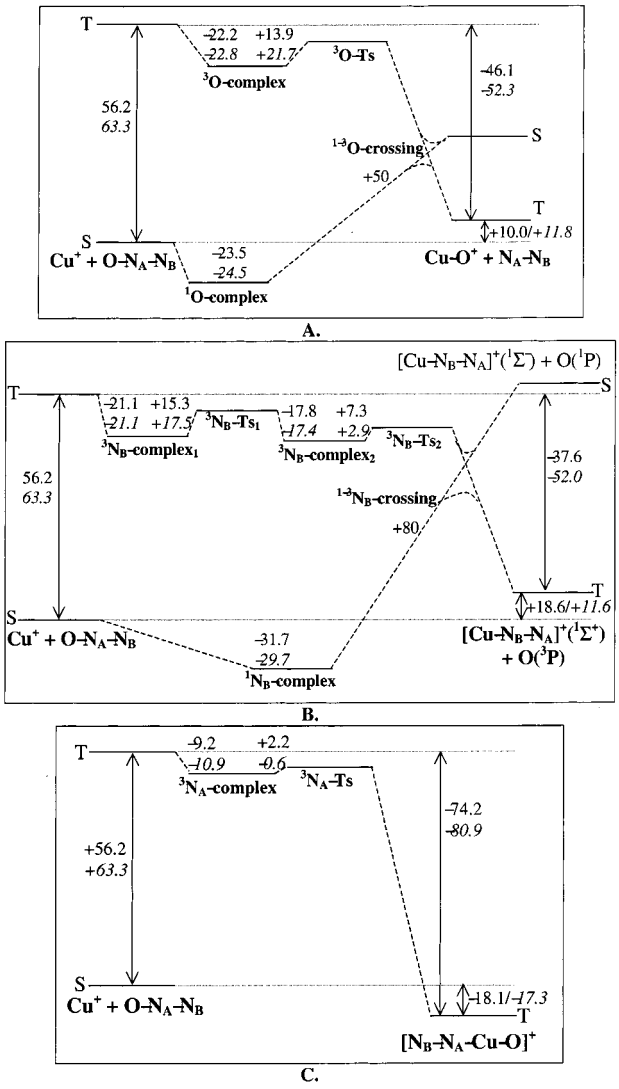

Figure 3. Calculated reaction paths, A. for reaction 1, B. for reaction 2 and C. for reaction 3. The labeling of the various Cu−N_2O-complexes and transition state structures is also indicated. Relative energies are indicated in kcal/mol. The upper values are obtained at the B3LYP level, while the lower values (in italics) were calculated by means of CCSD(T) at the B3LYP structures.

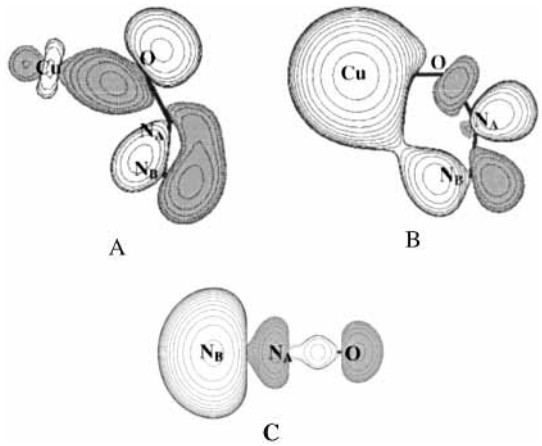

Figure 4. A and B: Orbital interactions in the ^{3}O-Ts structure (see also Figures 2 and 3). A. σ[Cu $3d_z^2$-N_2O HOMO-in-plane] interaction, B. σ[Cu 4s−N_2O LUMO-in-plane]. C. N_2O σ lone pair.

energy difference between the ^{3}O-complex and ^{3}O-Ts, is reported in Table 2. DFT predicts a much smaller energy barrier

TABLE 2: Binding and Reaction Energies and Activation Barriers for Reactions of Cu^+ with N_2O at the DFT-B3LYP Level and with CCSD(T) (All Energies Are Given in kcal/mol)

	B3LYP	CCSD(T)
O-attack		
B. E.[a] ^{3}O-complex	−22.2	−22.8
barrier ^{3}O-Ts	+13.9	+21.7
R. E.[b] ($^3Cu^+ + {}^1N_2O \rightarrow {}^3CuO^+ + {}^1N_2$)	−46.1	−51.8
B. E. ^{1}O-complex	−23.5	−24.5
barrier $^{1-3}$crossing$^+$	+40	
R. E. ($^1Cu^+ + {}^1N_2O \rightarrow {}^3CuO^+ + {}^1N_2$)	+10.0	+11.8
N_B-attack		
B. E. ^3N_B-complex$_1$	−21.1	−21.1
barrier ^3N_B-Ts$_1$	+15.3	+17.4
B. E. ^3N_B-complex$_2$	−23.4	−21.0
barrier ^3N_B-Ts$_2$	+7.3	+2.9
R. E. ($^3Cu^+ + {}^1N_2O \rightarrow {}^1CuN_2^+ + {}^3O$)	−37.6	−51.9
B. E. ^1N_B-complex	−31.7	−29.7
barrier $^{1-3}$crossing$^+$	+80	
R. E. ($^1Cu^+ + {}^1N_2O \rightarrow {}^1CuN_2^+ + {}^3O$)	+18.6	+11.7
N_A-attack		
B. E. ^3N_A-complex	−9.2	−10.9
barrier ^3N_A-Ts	+2.2	−0.6
R. E. ($^3Cu^+ + {}^1N_2O \rightarrow {}^3[OCuN_2]^+$)	−74.2	−81.3

[a] B. E. = binding energy. [b] R. E. = reaction energy.

(13.9 kcal/mol) than that predicted by CCSD(T) (21.7 kcal/mol). These barriers are relatively large, but note that they are still smaller than the barrier that must be overcome to return to the initial reagents (see Figure 3A). These high energy barriers are much larger than those encountered in the reaction of neutral Cu atoms with N_2O, where values below 5 kcal/mol were calculated.[24]

$^1Cu^+ + {}^1N_2O \rightarrow {}^3CuO^+ + {}^1N_2$. If N_2O approaches the ground state $^1Cu^+$ ions via its oxygen side, a complex is also formed first (indicated as ^{1}O-complex in Figure 3A), about 23−24 kcal/mol more stable than the initial singlet reagents. The structure of this complex is similar to that of the ^{3}O-complex, with a linear N_2O system and a Cu−O−N_A angle of about 130 degrees. However, the Cu−O bond length is shorter than in the case of the excited state $^3Cu^+$-complex, because of the absence of 4s-ligand repulsion. We have also calculated the structure of a linear O-side $^1Cu^+$−N_2O-complex by imposing $C_{\infty v}$ symmetry in the DFT geometry optimizations. As for the linear ^{3}O-complex, this stationary point was characterized by two (equal) negative frequencies, corresponding to the bending vibrations of the Cu−O−N angle. However, the energy of the singlet saddle point was only 1.5 kcal/mol higher than that of the bent minima, as compared to an energy difference of 6.0 kcal/mol for the corresponding triplet structures. This is obviously due to the absence in the ^{1}O-complex of stabilizing forces connected with N_2O HOMO → Cu^+ $3d_z^2$ σ-donation (cfr Figure 4A). We also note that the isoelectronic $^1Cu^+$−CO_2-complex was reported to be linear.[9] The binding energies of N_2O and CO_2 to $^1Cu^+$, about 22−24 kcal/mol, are in the same energy range.[9]

The formation of the $^3CuO^+ + N_2$ reaction products out of ^{1}O-complex involves a change of spin and must therefore proceed through a crossing point of the singlet and triplet surfaces. To obtain an estimate of the energy barrier of the reaction, we have attempted to calculate the structure of the singlet−triplet crossing point in the following way: Defining the O−N_A bond distance as the reaction coordinate, the structure of the singlet state was obtained at several points along the reaction path, by keeping only the latter distance fixed (between 1.2 and 2.0 Å) and optimizing all other geometrical parameters. A single-point energy calculation of the triplet state was then

performed at each of these structures. As such, a singlet−triplet crossing was observed, at an O−N distance of 1.79 Å. The estimated energy barrier from these calculations for reaction starting from the singlet complex is 50 kcal/mol, i.e., considerably higher than the reaction energy. Please note that this result represents an upper bound, since the triplet surface was not explored. It is interesting to compare this energy barrier to the one for the N_2O decomposition reaction with $^1Cu^+$ ions bound to zeolite surfaces. This barrier was recently estimated to be 23 kcal/mol, by means of DFT calculations on cluster models.[36] This substantial reduction of the barrier indicates that the zeolite matrix may indeed exert a strong catalytic effect on the above reaction.

$^3Cu^+ + {}^1N_2O \rightarrow {}^1CuN_2^+ + {}^3O$. We will now consider the reaction between Cu^+ and the terminal nitrogen (N_B) of N_2O, leading to the formation of CuN_2^+ and O (reaction). CuN_2^+ has a $^1\Sigma^+$ ground state, while the O atom has a ^3P ground state. From the reaction paths presented in Figure 3B, one can see that the formation of these products is again exothermic and spin-allowed for the $^3Cu^+$ cations, but not for $^1Cu^+$.

The reaction of $^3Cu^+$ with N_2O again starts with the formation of a complex. Two different structural minima were optimized. The first complex, denoted as ^3N_B-complex$_1$ in Figures 2 and 3B, has a linear structure. Its binding energy (−21.1 kcal/mol) is slightly smaller than that of ^{3}O-complex. The second N_B-side complex, denoted as ^3N_B-complex$_2$, has about the same binding energy. Here, both Cu−N_B−N_A and O−N_A−N_B angles are bent. A Mulliken orbital population analysis reveals that the electronic structure of ^3N_B-complex$_2$ is completely different from that of ^{3}O-complex and ^3N_B-complex$_1$. The electronic configuration of Cu is $3d^{10}$ instead of $3d^94s^1$, indicating that the main part of the spin density has been shifted to N_2O. The ^3N_B-complex$_2$ can thus be viewed as arising from an interaction between a $^1Cu^+$ cation and ^3N_2O. The absence of electrons in the 4s orbital explains the much shorter Cu−N distance in the ^3N_B-complex$_2$ (1.846 Å) as compared to that in the ^3N_B-complex$_1$ (2.077 Å). The triplet multiplicity of N_2O explains why the O−N_A−N_B bond angle is bent: the structure of ^3N_2O (shown in Figure 1) indeed displays a bond angle of 122 degrees, almost the same as in ^3N_B-complex$_2$. Excitation to the N_2O triplet state weakens both the O−N and N−N bonds, as an electron is transferred from the nonbonding π HOMO the antibonding π° LUMO. The singly occupied N_2O HOMO and LUMO orbitals are situated in the symmetry plane of the ^3N_B-complex$_2$ and interact with the fully occupied 3d orbitals on Cu. The occurrence of a complex in which the spin density is shifted toward N_2O is not surprising considering that the singlet−triplet excitation energies of Cu^+ and N_2O both lie within the same energy range. The N_2O singlet−triplet excitation energy was calculated at 67.0 and 69.7 kcal/mol for the B3LYP and CCSD(T) levels of theory, respectively. This is indeed very close to the singlet−triplet splitting for Cu^+ (see Table 1).

Between the ^3N_B-complex$_1$ and ^3N_B-complex$_2$, a transition state (^3N_B-Ts$_1$) was calculated, 15.3 kcal/mol (at the DFT level) higher in energy than ^3N_B-complex$_1$. This relatively large energy barrier can be overcome with the excess energy gained in the formation of the ^3N_B-complex$_1$ (see Figure 3B). The formation of the $^1CuN_2^+$ and ^3O reaction products out of the ^3N_B-complex$_2$ is then straightforward. The spin density accumulates on oxygen while the O−N bond length increases. The O−N_A-N_B angle is bent further, while the Cu−N_B−N_A angle is enlarged in order to create the linear $[Cu-N_2]^+$-complex. The DFT energy barrier is 7.3 kcal/mol, but this barrier reduces to only 2.9 kcal/mol at the CCSD(T) level.

$^1Cu^+ + {}^1N_2O \rightarrow {}^1CuN_2^+ + {}^3O$. The reaction path of $^1Cu^+$ cations with N_2O is similar to that of the reaction at the oxygen side of N_2O: it is also endothermic and spin-forbidden. First, a singlet complex is formed. This ^1N_B-complex is found to be linear. The σ lone pair of N_2O has a much larger lobe on the N-side than on the O-side (see Figure 4C) resulting in linear coordination via N_B. This is also reflected in the binding energy of N_2O (see Table 2), which is substantially larger than that of the ^{1}O-complex. The point of intersection between singlet and triplet surfaces along the reaction coordinate was estimated with an energy barrier of 80 kcal/mol, much larger than the reaction energy. Closed-shell $^1Cu^+$ cations thus appear to be inert with respect to N_2O-attack.

$^3Cu^+ + {}^1N_2O \rightarrow {}^3OCuN_2^+$. Finally, we have considered the possibility of reaction of Cu^+ with N_2O via an attack of the central nitrogen (N_A) (reaction). As indicated in Figure 3C, such a reaction path was found only for ^3D Cu^+ ions but not for ^1S Cu^+ ions.

Before moving to the transition state, another $[Cu-N_2O]^+$-complex is formed, denoted as ^3N_A-complex (see Figures 2 and 3C). The N_2O system is bent, due to the fact that the spin density is mainly concentrated on the N_2O system, not on Cu^+. Indeed, the orbital occupation numbers again point to a Cu^+ $3d^{10}$ configuration, as for the ^3N_B-complex$_2$. The binding energy of the ^3N_A-complex is somewhat lower than that of the O− or N_B-end triplet complexes: about 9−11 kcal/mol, as opposed to more than 20 for the other complexes. This is also reflected in the structure: the Cu−N bond distance is much longer in the ^3N_A-complex as compared to the N_B-complex$_2$ (see the structures in Figure 2).

The structure of the transition state is very close to that of the complex. The spin density is further transferred toward O, while the O−N bond length increases. After the transition state, the oxygen moves in the direction of Cu^+. As such, the Cu^+ ion is inserted in the O−N bond. The energy barrier calculated for this reaction is very low both for DFT and CCSD(T). The barrier almost vanishes at the CCSD(T) level of theory.

As shown in section 3.1, the $^3OCuN_2^+$-complex is the most stable reaction product of the Cu^+-N_2O reactions. We note that this product can also be formed from the recombination of CuO^+ and N_2, formed in reaction 1, or out of CuN_2^+ and O, formed in reaction 2. Our calculations indicated no reaction barriers for these recombination reactions. On the other hand, the question remains whether the $^3[OCuN_2]^+$-complex, formed in reaction 3, can have a significant lifetime. The number of degrees of freedom to distribute the large excess of reaction energy is small. It is the question whether the insertion product can be stabilized by thermal collisions or whether it will dissociate for example to CuO^+ and N_2 or $[CuN_2]^+$ and O, about 30−40 kcal/mol higher in energy. Rodgers et al. indeed observed the formation of a $[CuN_2O]^+$ adduct at thermal energies, and suggested that this adduct is formed by collisional stabilization in sequential bimolecular reactions.

4. Conclusions

The ab initio study of the reactions of $^1Cu^+$ and $^3Cu^+$ ions with N_2O demonstrates that $^1Cu^+$ ions are relatively inert with respect to N_2O reactions, while $^3Cu^+$ ions are highly reactive. Three reaction channels have been analyzed. If N_2O approaches the Cu^+ ions via its O-side, this leads to formation of CuO^+ and N_2. On the other hand, if N_2O attacks via its N-end, the reaction products are CuN_2^+ and an O atom. Finally, we found that Cu^+ atoms in the ^3D state can also react with N_2O via the central nitrogen, leading to insertion of Cu^+ in the O−N_2 bond,

with formation of $[OCuN_2]^+$. The latter reaction is the most exothermic reaction. The reactions of $^1Cu^+$ ions proceed with high energy barriers; the lowest energy barrier (50 kcal/mol) is encountered for the formation of CuO^+ and N_2. On the other hand, all reactions of $^3Cu^+$ ions are barrierless. These results are in agreement with the experimental findings.

The reaction and binding energies and energy barriers calculated with DFT and CCSD(T) are in reasonable agreement with each other and experimental data (where available) in the case of reactions involving Cu−N bonds. On the other hand, we have found significant differences between the DFT and CCSD(T) results for reactions in which a Cu−O bond is formed or broken.

Acknowledgment. This investigation has been supported by grants from the Flemish Science Foundation (FWO) and from the Concerted Research Action of the Flemish Government (GOA).

References and Notes

(1) Homma, K.; Nakamura, M.; Clemmer, D. E.; Koyano, I. *J. Phys. Chem.* **1994**, *98*, 13286−13293.
(2) Plane, J. M. C.; Rollason, R. J. *J. Chem. Soc., Faraday Trans.* **1996**, *92*, 4371.
(3) Ritter, D.; Carroll, J. J.; Weisshaar, J. C. *J. Phys. Chem.* **1992**, *96*, 10636.
(4) Campbell, M. L.; Kölsch, E. J.; Hooper, K. L. *J. Phys. Chem. A* **2000**, *104*, 11147.
(5) Futerko, P. M.; Fontijn, A. *J. Chem. Phys.* **1991**, *95*, 8065.
(6) Thomas, J. L. C.; Bauschlicher, C. W.; Hall, M. B. *J. Phys. Chem. A* **1997**, *101*, 8530−8539.
(7) Hendrickx, M.; Ceulemans, M.; Gong, K.; Vanquickenborne, L. *J. Phys. Chem. A* **1997**, *101*, 8640−8546.
(8) Kushto, G. P.; Zhou, M.; Andrews, L.; Bauschlicher, C. W. *J. Phys. Chem. A* **1999**, *103*, 1115−1125.
(9) Sodupe, M.; Branchadell, V.; Rosi, M.; Bauschlicher, C. W. *J. Phys. Chem. A* **1997**, *101*, 7854.
(10) Bauschlicher, C. W.; Zhou, M.; Andrews, L.; Johnson, J. R. T.; Panas, I.; Snis, A.; Roos, B. O. *J. Phys. Chem. A* **1999**, *103*, 5463−5467.
(11) Rodgers, M. T.; Walker, B.; Armentrout, P. B. *Int. J. Mass Spectrom.* **1999**, *182*−*183*, 99.
(12) Armentrout, P. B.; Halle, L. F.; Beauchamp, J. L. *J. Chem. Phys.* **1982**, *76*, 2449−2457.
(13) Wiesenfeld, J. R.; Yuen, M. J. *Chem. Phys. Lett.* **1976**, *42*, 293.
(14) Ritter, D.; Weisshaar, J. C. *J. Phys. Chem.* **1989**, *93*, 1576.
(15) Ritter, D.; Weisshaar, J. C. *J. Phys. Chem.* **1990**, *94*, 4907.
(16) Narayan, S. A.; Futerko, P. M.; Fontijn, A. *J. Phys. Chem.* **1992**, *96*, 290.
(17) Futerko, P. M.; Fontijn, A. *J. Chem. Phys.* **1993**, *98*, 7004.
(18) Campbell, M. L.; McClean, R. E. *J. Phys. Chem.* **1993**, *97*, 7942.
(19) Campbell, M. L.; McClean, R. E. *J. Chem. Soc., Faraday Trans.* **1995**, *91*, 3787.
(20) Campbell, M. L. *J. Chem. Phys.* **1996**, *104*, 7515.
(21) Campbell, M. L.; Metzger, J. R. *Chem. Phys. Lett.* **1996**, *253*, 158.
(22) McClean, R. E.; Campbell, M. L.; Goodwin, R. H. *J. Phys. Chem.* **1996**, *100*, 751.
(23) Stirling, A. *J. Phys. Chem. A* **1998**, *102*, 6565.
(24) Delabie, A.; Vinckier, C.; Flock, M.; Pierloot, K. *J. Phys. Chem. A* **2001**, *105*, 5479.
(25) Kapteijn, F.; Rodiguez-Mirasol, J.; Moulijn, J. A. *Appl. Catal., B* **1996**, *9*, 25.
(26) Nakao, Y.; Hirao, K.; Taketsugu, T. *J. Chem. Phys.* **2001**, *114*, 7935.
(27) Dolg, M.; Wedig, U.; Stoll, H.; Preuss, H. *J. Chem. Phys.* **1987**, *86*, 866.
(28) Schäfer, A.; Huber, C.; Ahlrichs, R. *J. Chem. Phys.* **1994**, *100*, 5829.
(29) Gonzalez, C.; Schlegel, H. B. *J. Phys. Chem.* **1990**, *94*, 5523.
(30) Pierloot, K.; Tsokos, E.; Roos, B. O. *Chem. Phys. Lett.* **1993**, *214*, 583.
(31) Widmark, P.-O.; Malmqvist, P.-Å.; Roos, B. O. *Theor. Chim. Acta*, **1990**, *77*, 291.
(32) Frisch, M. J.; Trucks, G. W.; Schlegel, H. B.; Scuseria, G. E.; Robb, M. A.; Cheeseman, J. R.; Zakrzewski, V. G.; Montgomery, J. A., Jr.; Stratmann, R. E.; Burant, J. C.; Dapprich, S.; Millam, J. M.; Daniels, A. D.; Kudin, K. N.; Strain, M. C.; Farkas, O.; Tomasi, J.; Barone, V.; Cossi, M.; Cammi, R.; Mennucci, B.; Pomelli, C.; Adamo, C.; Clifford, S.; Ochterski, J.; Petersson, G. A.; Ayala, P. Y.; Cui, Q.; Morokuma, K.; Malick, D. K.; Rabuck, A. D.; Raghavachari, K.; Foresman, J. B.; Cioslowski, J.; Ortiz, J. V.; Stefanov, B. B.; Liu, G.; Liashenko, A.; Piskorz, P.; Komaromi, I.; Gomperts, R.; Martin, R. L.; Fox, D. J.; Keith, T.; Al-Laham, M. A.; Peng, C. Y.; Nanayakkara, A.; Gonzalez, C.; Challacombe, M.; Gill, P. M. W.; Johnson, B. G.; Chen, W.; Wong, M. W.; Andres, J. L.; Head-Gordon, M.; Replogle, E. S.; Pople, J. A. *Gaussian 98*, revision A.5; Gaussian, Inc.: Pittsburgh, PA, 1998.
(33) Andersson, K.; Barysz, M.; Bernhardsson, A.; Blomberg, M. R. A.; Cooper, D. L.; Fleig, T.; Fülscher, M. P.; de Graaf, C.; Hess, B. A.; Karlström, G.; Lindh, R.; Malmqvist, P.-Å.; Neogrády, P.; Olsen, J.; Roos, B. O.; Sadlej, A. J.; Schütz, M.; Schimmelpfennig, B.; Seijo, L.; Serrano-Andrés, L.; Siegbahn, P. E. M.; Stålring, J.; Thorsteinsson, T.; Veryazov, V.; Widmark, P.-O. *MOLCAS*, version 5; Department of Theoretical Chemistry, Chemistry Center, University of Lund: P.O. Box 124, S-221 00 Lund, Sweden, 1997.
(34) Lide, D. R., Ed. *CRC Handbook of Chemistry and Physics*, electronic version; CRC Press: Boca Raton, FL, 1999.
(35) Moore, C. E. *Atomic Energy Levels, as Derived from the Analyses of Optical Spectra*; U.S. Government Printing Office: Washington, DC, 1952.
(36) Sengupta, D.; Adams, J. B.; Schneider, W. F.; Hass, K. C. *Catal. Lett.* **2001**, *74*, 193.
(37) Luna, A.; Alcam×c1, M.; Mó, O.; Yáñez, M. *Chem. Phys. Lett.* **2000**, *320*, 129−138.
(38) Bauschlicher, C. W.; Maitre, P. *Theor. Chim. Acta* **1995**, *90*, 189.
(39) Pierloot, K. To be published.
(40) Fiedler, A.; Schröder, D.; Shaik, S.; Schwarz, H. *J. Am. Chem. Soc.* **1994**, *116*, 10734.